Wind Turning in The Atmospheric Boundary Layer

Master's thesis in Physics and Astronomy

GHAZAL TORABI

Department of Fundamental Physics
Division of Physics and Astronomy
CHALMERS UNIVERSITY OF TECHNOLOGY
Göteborg, Sweden 2013
Master's thesis 2013:68

MASTER'S THESIS IN PHYSICS AND ASTRONOMY

Wind Turning in The Atmospheric Boundary Layer

GHAZAL TORABI

Wind Turning in The Atmospheric Boundary Layer
GHAZAL TORABI

Cover:
A contour plot of an average diurnal wind turning from height 40 to 200 m by lidar observations

Wind Turning in The Atmospheric Boundary Layer
Master's thesis in Physics and Astronomy
GHAZAL TORABI
Department of Fundamental Physics
Division of Physics and Astronomy
Chalmers University of Technology

Abstract

Measurements at Høvsøre site in Denmark are used to analyse the change with height of wind speed and the turning of the wind in the atmospheric boundary layer. The purpose is to study the behaviour of wind turning and wind shear and analyse the relations between them.

The study will show the effect of wide range of stability classes on the turning of wind and wind speed by combining cup, wind vane and sonic at meteorological mast with lidar observations. Easterly wind is investigated at Høvsøre site to study the behaviour of the overland wind shear and wind turning from November 2008 to April 2009. In this study, data are analysed based on average 10-min wind speeds and wind directions diurnal, monthly and during the whole period of measurements.

The results show that first, the wind speed profile of meteorological mast and lidar are in agreement to different stability classes. Second, the wind direction profile changes with height reasonable in all stability conditions except in very unstable and unstable cases. Third result shows that the wind shear and the wind turning are unstable during the day and stable during the night in the average whole period of six months. Fourth, the yearly wind turning and wind shear are in agreement without considering lidar observations. They behave also in similar way when lidar observations combine with meteorological mast. In conclusion, the comparisons between the wind shear and the turning of the wind with and without considering lidar observation show that the wind shear is in the agreement with the wind turning.

The second result on this study was unexpected. The reason for this behaviour may be explained as the number of measurements are very low. Another reason is that the value of heat fluxes are low, whereas they have to be high. The last reason might be related to a baroclinicity.

Keywords: Wind shear, Surface layer, Turbulence

Preface

This thesis was prepared at the department of Wind Energy at the Technical University of Denmark in fulfilment of the requirements for acquiring an M.Sc. in Physics and Astronomy. This master thesis was conducted during the final year of my two years Master of Science program in Physics and Astronomy. My work has been carried out in the Meteorological section at the DTU wind energy - Risø; under the supervision of Jacob Berg. Alfredo Peña served as co-supervisor.

This thesis deals with the changes in the wind speed and the wind direction in the atmospheric boundary layer by combining cup, sonic and vane at meteorological mast with lidar observations overland at Høvsøre, Denmark. This study is carried out by averaging the 10-min wind speed and wind direction measurements in the wide range of atmospheric stability conditions from November 2008 to April 2009.

This thesis includes 7 main sections. Section 1 is the introduction. Section 2 provides a review of the main characteristics of the atmospheric boundary layer, including the effect of stability and turbulence in the surface. It also shows how the analysis of the turning of the wind has been performed. Section 3 provides a description of the Høvsøre site in Denmark and the instrumentation used in this study. Section 4 explains data filtering and data averaging. Section 5 provides the results from the analysis of both wind shear and the turning of the wind. Discussion and conclusions are provided in the last two sections.

Acknowledgements

CONTENTS

List of Figures

List of Tables

Notation

d	focused distance
d'	distance from laser source to targets in air
u_*	friction velocity
w_0	angular frequency of light
Δf	Doppler shift
γ	latitudinal component of geostrophic wind
∂	partial derivative
θ	wind direction
θ'	potential temperature
λ_l	wavelength of light
ϕ	the angle when the laser beam tilt from the zenith
ψ_m	diabatic correction of the logarithmic wind profile
σ_θ	standard deviation
φ_m	dimensionless wind shear
φ	along-beam weighting function
Dir	horizontal wind direction
g	gravitational acceleration
K_M	turbulent exchange coefficient for momentum
Q_0	heat flux
R^2	determination coefficient
T_0	surface air temperature
u_g	longitudinal component of geostrophic wind
v_g	latitudinal component of geostrophic wind
V_h	horizontal wind speed
v_r	radial velocity
z_0	roughness length
z_i	height of boundary layer
f	Coriolis parameter
k	von Kármán constant
L	Obukhov length
n	number of measurements
U	mean wind speed
u	longitudinal component of wind speed
v	latitudinal component of wind speed
w	vertical component of wind speed
z	height above the ground
ABL	Atmospheric boundary layer
CBL	Convective boundary layer
DBS	Doppler beam swinging
SBL	Stable boundary layer
VAD	velocity azimuth display

1   Introduction

The behaviour of the atmospheric flow close to the ground's surface is a main concern in wind energy [BMN13]. The ground's surface has an effect on the wind characteristics even at altitudes above 100 m [Ass00]. The wind is influenced by roughness, roughness changes, terrain, and obstacles, as many of these terrain and surface characteristics add/subtract drag to the flow. Hence, the wind speed and wind direction profile at various heights above the ground level depend on the surface topology, atmospheric stability and changes in time. [DN09].

Wind turbines have increased in size in the last two decades due to high demand for wind power. This growing in size causes environmental and economical impacts. From the economic point of view, the cost of energy has decreased. The reason is that the industries have based their investments on acknowledge component of the power generation which in the wind energy depends on the wind characteristics [Ass+09]. Atmospheric stability can affect the wind speed and wind direction thus affecting power generation. This impact has had different results in several studies. For example, Rareshide et al (2009) found high wind shear (stable condition) makes the higher power production than low wind shear (unstable condition) at a US plains wind farm [Rar+09]. In contrast, Wagner et al (2009) found high wind shear lead to lower power than low wind shear in the flat Danish terrain [Wag+09],[WL12].

Atmospheric turbulence can have significant effects on the turbines and environment. It affects turbine loads through fatigue and wake effects. In a wind farm, turbines themselves create turbulence in their wakes and this turbulence is added to atmospheric turbulence and increases the load. Another impact is related to the increase in propagation of noise from the wind turbines themselves. Under unstable conditions, strong turbulence creates background noise near the ground surface and so the noise from the turbines is negligible. By contrast, the turbine noise is heard more clearly in the stable condition [LC12].

The large turbines cause meteorological features which have not been considered in the past are playing a main role. For instance, the vertical gradient of mean wind speed or the analysis of the wind turning has not been include in many studies [Etl02]. In particular, the wind turning has not been so important as people tend to believe that close to the surface the wind does not turn too much. However, with the modern wind turbines, wind turning may be as important as the wind shear. The vertical wind profile varies through time and space and so it is important to observe the wind characteristics as accurately as possible [DN09]. Furthermore, collecting wind information from these tall turbines need new techniques, i.e. remote sensors, because the installation of the meteorological mast above 80 m becomes expensive. By measuring with different instruments, part of the uncertainty of the results of the analysis can be evaluated as the three types of the instruments observe the wind speed and wind direction in a different manner.

Accurate prediction of the wind speed and the wind direction is extremely important for the wind energy industry. For example, high accuracy decreases the uncertainty of the predicted energy production [Ass+09]. If wind conditions evolve differently than expected, companies face financial losses, production and sales difficulties.

The main goal of this project, which has been carried out at DTU Wind Energy, Risø campus, is to study the variation with height (i.e. the vertical profile) of both the turning of the wind and the vertical wind speed in the atmospheric boundary layer from the analysis of cup and sonic anemometer measurements combined with wind lidar observations at a flat area known as Høvsøre in Western Denmark. The vertical wind speed profiles and profiles of the wind turning are analysed under a wide range of atmospheric stability conditions for the different instruments as it has been observed that these profiles show distinctive shape and behaviour depending on the atmospheric turbulence characteristics [Sat+12], [SM09].

This thesis includes 7 main sections. Section 2 provides a review of the main characteristics of the atmospheric boundary layer, including the effect of stability and turbulence on the surface. It also shows how the analysis of the turning of the wind has been performed. Section 3 provides a description of the Høvsøre site in Denmark and the instrumentation used in this study. Section 4 explains about the data filtering and data averaging. Section 5 provides the results of the analysis of both wind shear and the turning of the wind. Discussion and conclusions are provided in the last two sections.

2 Theory

2.1 The Atmospheric Boundary Layer

The atmospheric boundary layer (ABL) is a part of the troposphere. The ABL is affected by turbulence motion and so its thickness varies between a hundred meter to a few kilometres [Stu88]. The characteristics of this layer are different during the day, in particular when it is warm, than during the night. This difference is explained firstly by wind shear, which is produced by friction of the wind with the surface, and secondly by the heat flux that is caused by the differences of temperature of the air layers and the surface. There are three main different turbulence regimes in which the atmospheric flow is commonly classified when the boundary layer is assumed to be homogeneous:

1. Convective or unstable: This occurs when the heat is transferred from the warm surface to the colder atmosphere. During the day the surface is warmer than the atmosphere, and the difference in density between the warm and the cold air gives rise to buoyancy forces in the atmosphere, causing unstable condition. Thus, the vertical motion in unstable atmosphere is large and the thickness of the layer reaches to one or two kilometres [Peñ09].

2. Neutral: This condition dominates when there is no net heat flux in the atmosphere, but with high friction velocity. It means that the wind speed is high near the surface [Peñ09]. Neutral condition is between unstable and stable conditions. It happens usually in the cloudy weather when strong surface heating and cooling do not occur [Sys13].

3. Stable: It is dominating when the surface is cool and there is a high wind shear. At night the surface is colder than the atmosphere and the colder air wants to stay in its position. The stable condition is also found over ice and snow that cover the surfaces. The vertical motion in the stable atmosphere happens rarely. Therefore, the thickness of layer is around a hundred meter [Peñ09].

Figure 2.1 shows the structure of the ABL during 24 hours. It consists of the surface layer, convective boundary layer (CBL), stable boundary layer (SBL), residual layer and entrainment zone. Unstable condition is dominating in the CBL and happens during the day. Besides, converting potential energy to kinetic energy causes an increase in the turbulence level. In the SBL, the temperature and wind speed are not constant contrary to CBL, and the the height of SBL is determined when the smaller eddies reach to the residual layer. Residual layer is located on the top of this layer which is made by CBL and the entrainment zone. In addition, the entrainment zone comes from the interaction of free stable atmosphere and CBL layer. The inversion happens in this part because the temperature and height have direct proportion [Peñ09].
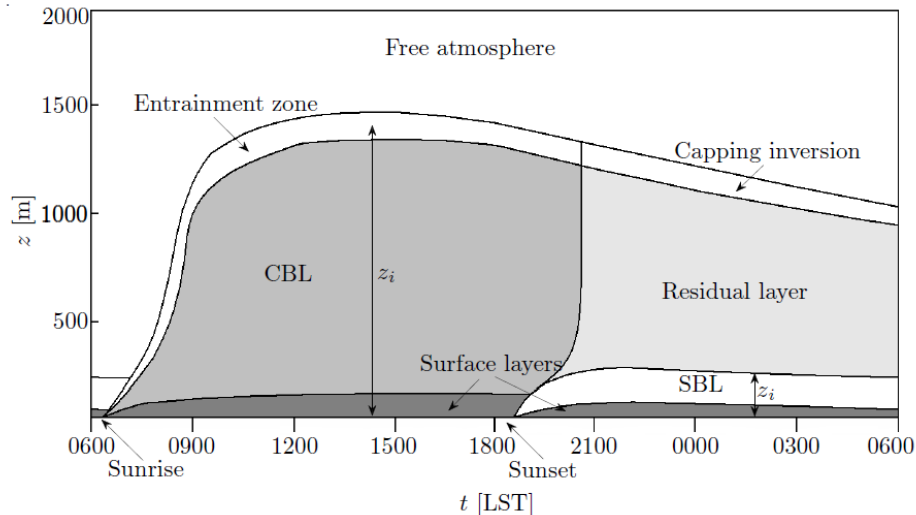
Figure 2.1: *The evolution of the atmospheric boundary layer with height during an ideal daily cycle. CBL and SBL are convective boundary layer and stable boundary layer respectively. z is the height from the ground and z_i is the boundary layer height [Peñ09].*

2.2 The Surface Layer

There is a region in the ABL called the surface layer, which has approximately constant vertical momentum, heat and moisture, and large temperature gradients and strong wind. Besides, the surface layer can extend from a few meters to hundred meters above the ground in various stability conditions [Peñ09]. Thus, the atmospheric characteristics will be discussed in this section.

The atmospheric stability conditions can be determined by the Obukhov length or the Richardson number. The Obukhov length scale, L is defined by the heat flux, $Q_0 = < w'\theta' >$ where w' and θ' are vertical component of velocity and potential temperature, respectively, by buoyancy, g/T_0 where g is the gravitational acceleration, T_0 is the surface air temperature, and by the friction velocity, u_* [Peñ09]. The friction velocity is defined as

$$u_*^2 = - < u'w' > \tag{2.1}$$

where u is the longitudinal and w is vertical wind speed component and prime denotes fluctuations [BMN13]. In the following, the length scale L is given as

$$L = \frac{-T_0 u_*^3}{kgQ_0} \tag{2.2}$$

where k = 0.4 is the von Kármán constant. When there is a stable condition, the heat flux is negative, which means the atmosphere is warmer than the surface. Hence, L is positive, since Q_0 and L has inverse relation. Furthermore, L is negative when the earth is releasing heat ($Q_0 > 0$) [BMN13]. The wind shear is defined as

$$\frac{du}{dz} = \frac{u_*}{kz}\varphi_m(z/L) \tag{2.3}$$

where z is the height above the ground, and φ_m is dimensionless wind shear that is a function of z/L, dimensionless stability. When $\varphi_m = 1$, the wind profile is neutral, which means $Q_0 = 0$ and then the integral of Eq. (2.3) will be

$$U = \frac{u_*}{kz}\ln(z/z_0) \tag{2.4}$$

where z_0 is the roughness length. The integral of Eq. (2.2) has a different form when wind profile is not neutral

$$U = \frac{u_*}{k}[\ln(z/z_0) - \psi_m] \tag{2.5}$$

where ψ_m is the diabatic correction of the logarithmic wind profile and it is the integrated form of the experimental function φ_m [Peñ09].
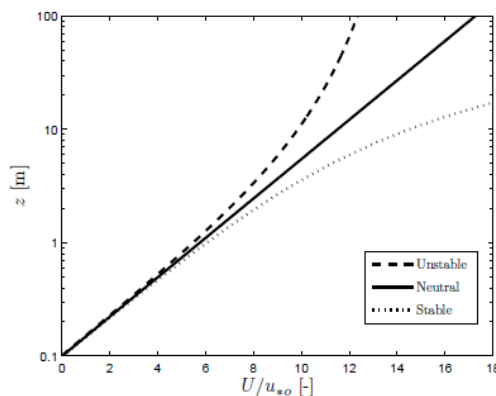
Figure 2.2: *The logarithmic behaviour of the wind profile in three stability conditions in the surface layer, z_0=0.1 m [Peñ09].*

Figure 2.2 shows the logarithmic behaviour of the wind profile in three main stability classes in the surface layer; that they are concluded from Eq. (2.5). The typical shapes of stable, neutral and unstable conditions are concave, straight line and convex, respectively. U/u_*, which makes the wind profile as a function of z/L and z/z_0.

2.3 The Ekman Spiral

The earth rotation causes an apparent deflection of the air path to the right in the Northern hemisphere. The force that causes this deflection is the Coriolis force. The Ekman spiral is a consequence of the Coriolis force. The Coriolis force acts on the transfer of moment from one layer of air to another [Ant00].

Large wind turbines with heights more than 100 m are partly in the Ekman layer. In the ABL over flat homogeneous terrain, the Ekman layer has been defined between the surface layer and free atmosphere when the Coriolis force, pressure gradient force and frictional force are in balance in the Ekman layer. The main difference between the surface layer and the Ekman layer is the behaviour of the turning of the wind with height. Thus, the behaviour of the wind in the Ekman layer has to be analysed. The following equations show when the Coriolis force, pressure gradient force and frictional force are in balance

$$-fv + fv_g - \frac{\partial}{\partial z}K_M\frac{\partial u}{\partial z} = 0 \qquad (2.6)$$

$$-fu + fu_g - \frac{\partial}{\partial z}K_M\frac{\partial v}{\partial z} = 0 \qquad (2.7)$$

where u_g and v_g are the longitudinal and latitudinal components of the geostrophic wind. u and v are the longitudinal and latitudinal components of the wind speed. f is the Coriolis parameter, and K_M (m^2/s) is the turbulent exchange coefficient for momentum [Etl02]. In order to analyse the behaviour of the vertical wind profile in the Ekman layer, the following equations are derived from Eq. (2.6) and Eq. (2.7)

$$u = u_g(1 - 2e^{-\gamma z}\cos(\gamma z)) \qquad (2.8)$$

$$v = u_g e^{-\gamma z}\sin(\gamma z) \qquad (2.9)$$

where $\gamma = \sqrt{\frac{f}{2K_M}}$ is the length scale. The inverse of this length scale estimates the top height of the Ekman layer, z_g [Amo06]. It is assumed that K_M is constant and at $z = o$, the geostrophic wind is $V_g = u_g$ and $v_g = 0$ [Dub04].

The wind vector from Eq. (2.8) and (2.9) are plotted for various heights, and it is concluded that the wind is deflected from the ground wind to the geostrophic wind which is known as the Ekman Spiral. It means that the air at the surface moves at an angle to the wind, and the air above the surface turns a bit more, and the air over that turns even more. Therefore, the wind rotates with height toward the geostrophic wind until the actual wind vector finally agrees with the geostrophic wind direction. This spiral forms as it is seen in figure 2.3. The angle between the ground wind and the geostrophic wind is called the angle of deflection. This angle varies with surface type from 10 to 45 degrees [Etl02]. As the Høvsøre site is the mostly covered by grass, the deviation angle varies around 15-25 (when $z_0 = 0.01$ and $u_* = 0.3$).
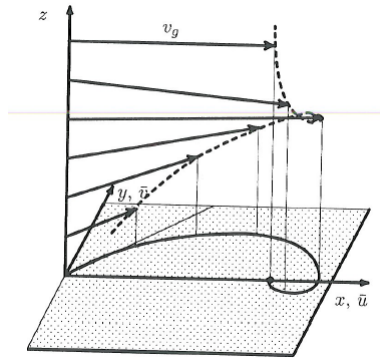
Figure 2.3: *The Ekman Spiral. u and v are the longitudinal and latitudinal components of wind speed. u_g and v_g are the longitudinal and latitudinal components of the geostrophic wind [Etl02].*

3 Site and Instrumentation

3.1 Høvsøre

The national test centre for large wind turbines in Denmark is at Høvsøre, which was established in 2002 on the West coast of Jutland. The North Sea is in the West side of Høvsøre site, and the continual wind comes from the West. Høvsøre site is flat and homogeneous and it is covered mostly by grass, crops and a few shrubs [Peñ09].

The meteorological mast is located in the South of the test site, which consists of cup and sonic anemometers, wind vanes and other meteorological sensors. At height 10 m, 40 m, 60 m, 80 m, 100 m and 116 m cup anemometers are situated for measuring wind speeds. Sonic measures parameters at heights 10 m, 20 m, 40 m, 60 m, 80 m and 100 m. Wind vane is available for measuring wind direction at 10 m, 60 m and 100 m. Besides, there is a 165 m light tower on the east of the site, and it has cup and sonic anemometers at three different heights of 60 m, 100 m and 160 m [Peñ09]. Both the light tower and meteorological mast are equipped with METEK scientific USA-1 sonic anemometers. In figure 3.1, the location of meteorological mast, wind turbines and light tower are illustrated. Easterly sector at Høvsøre is considered to study and analyse the wind profile over the land. The distribution of Easterly wind is between the direction 65 and 125 degrees from the geographical North.
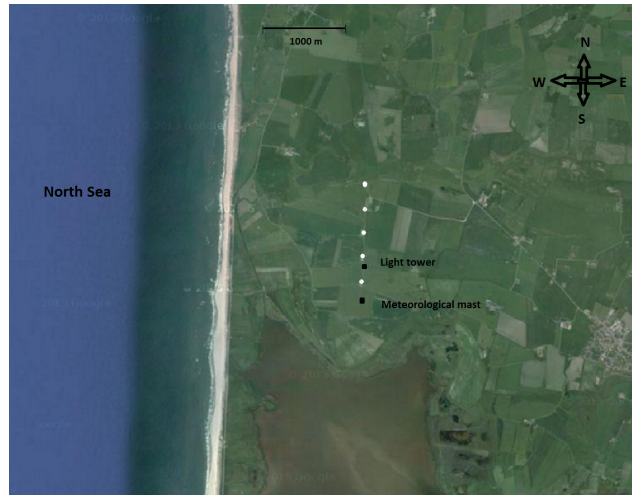
Figure 3.1: *Høvsøre national test centre for large wind turbines at Denmark. Light tower and meteorological mast are shown in the figure. 5 white dots are wind turbines.*

3.2 Instrumentation

3.2.1 Lidar

Remote sensors are instruments to observe wind characteristics and detect energy reflected from the atmospheric particles. Lidar transmits a beam of light from a laser to the aerosol particle, which are moving at the wind speed. These particles are small and light to move at the true wind speed. The light interacts with the particle and a small fraction of it is scattered back to a detector. The wavelength of light, λ_l is shifted by the movement of the particle, and this effect is known as a Doppler shift, Δf. The relation between radial velocity, v_r of the particle, the Doppler shift and the wavelength of light is

$$v_r = \frac{\lambda_l \Delta f}{2} \tag{3.1}$$

The distance d between the laser and the particle is showin in figure 3.2. The contributions of the particle are weighted by function φ at distance d' [Peñ09].

There are some plausible sources of error in lidar. These errors can depend on: the laser wavelength, the background light, the aerosol concentration, resolution and range, the validity of lidar calibration procedures, and the uncertainty of the atmospheric transmission lidar profile at the lidar location [Phi79].
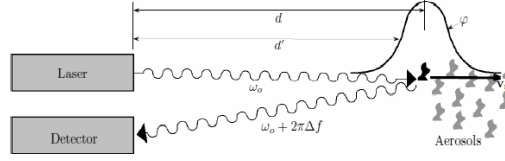
Figure 3.2: *Measurement process of the wind lidar. w_0 and Δf are frequency of light and Doppler shift, respectively. d shows the distance between a target and a laser. The moving target distance is shown by d' [Peñ09].*

In this study, the lidar WindCube version 1 is used, which is a pulsed lidar. The pulsed lidars provide radial wind components on various lines of sight at different heights. The scanning configuration can be according to velocity azimuth display (VAD) or Doppler beam swinging (DBS). DBS is used in pulsed lidars, can scan radial wind components on different points. The WindCube lidar scans the velocity at four points, separated by 90° (figure 3.3), in the following equations

$$v_r N = u\sin\phi + w\cos\phi, \text{for} \theta = 0° \tag{3.2}$$

$$v_r E = v\sin\phi + w\cos\phi, \text{for} \theta = 90° \tag{3.3}$$

$$v_r S = -u\sin\phi + w\cos\phi, \text{for} \theta = 180° \tag{3.4}$$

$$v_r W = -u\sin\phi + w\cos\phi, \text{for} \theta = 270° \tag{3.5}$$

where ϕ is the angle when the laser beam tilt from the zenith. u, v and w are wind speed components along the x-, y-, z- directions. They can be retrieved as [Car13b]

$$u = \frac{v_r N - v_r S}{2\sin\phi} \tag{3.6}$$

$$u = \frac{v_r E - v_r W}{2\sin\phi} \tag{3.7}$$

$$u = \frac{v_r N + v_r S + v_r E + v_r W}{4\cos\phi} \tag{3.8}$$

Horizontal wind speed, V_h and wind direction, Dir are computed as [Car13a]

$$V_h = \sqrt{u^2 + v^2} \tag{3.9}$$

$$Dir = \text{mod}(360° + \text{atan2}(u, v), 360°) \tag{3.10}$$

The lidar WindCube v1 collects measurements from heights 40 m to 300 m, but in this study, data from heights 40 m to 200 m is used, in order to have more accurate measurements.

3.2.2 Cup and Vane

John Thomas Romney Robinson in 1846 invented a simple anemometer, which had four cups. The angles between all cups are equal, and they are mounted vertically. The air flow in horizontal direction causes the cups to turn with speed proportional to the wind speed. Later, the three cups anemometer was invented, and this type of anemometer is currently used in wind energy industry. Therefore, the cup anemometer consists of three or four cups mounted symmetrically around a vertical shaft. The cup turns based on different pressure
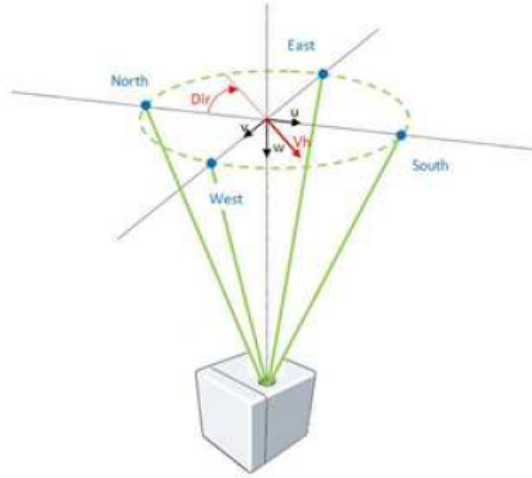
Figure 3.3: *Retrieving the wind speed components in lidar WindCube. u, v and w are the wind speed components. V_h and Dir show the horizontal wind speed and wind direction, respectively [Car13a].*

between the convex and concave side. The direction of turning is from convex side to concave side of the next cup. The cups are made of light alloy or carbon fiber thermo-plastic in recent years. Furthermore, the edges of the cups have beads to increase stiffness and preventing the effect of turbulence [Age12]. The cup anemometers have some disadvantages. They show higher mean wind speed than the true average wind speed in fluctuating wind. Another disadvantage is that they have low ability to provide accurate display of the changes in high wind speed fluctuations [Hun99]. In the present study, cup anemometers at heights 40 m, 60 m, 80 m, 100 m and 116 m are used to measure wind speed.

Wind vane and aero vane are two types of vanes. The difference between them is that the aero vane is used with propeller anemometer and a wind direction plate, whereas the wind vane is used alone. Quick changes in the wind direction has effect on the response of the wind vanes and the propeller anemometers. Therefore, this delay makes a significant error in observations [Age12]. Wind vane is available at heights 10 m, 60 m and 100 m at Høvsøre site.

3.2.3 Sonic

Sonic anemometers are used in measuring wind speed and wind direction based on ultrasonic sound waves. There are two pairs of sonic transmitting and receiving devices fixed facing each other. Each of these pairs send out ultra sonic wave pulse signals repeatedly at a certain time interval [Age12]. The modern sonic anemometers are used in the turbulent atmospheric boundary layer. This characteristic is the advantage of sonic than vane and cup. It means sonic anemometers have more quick response to the wind direction and wind speed variation than cup and vane [Hun99]. The current sonic anemometer has a disadvantage, that uses sensing heads whose geometry triggers some level of flow distortion which can cause wind speed errors [Hun99]. The sonic anemometers are located at heights 10 m, 20 m, 40 m, 60 m, 80 m and 100 m at Høvsøre. The measurements at height 40 m do not consider in this study, due to have many errors.

Cup, vane and sonic have some disadvantages related to their placement. They are mounted at different heights of the mast with low accuracy with the same offset at all heights. It means that all instruments at various heights have not been installed exactly in the same direction, i.e. in to the North. Another drawback is that mast installation becomes expensive for heights above 80 m. In contrast, lidar has one reference that scatters light to the atmosphere and so the offset at all heights are the same. Furthermore, lidar is less expensive with the same accuracy as cup and sonic anemometers for wind speed [Peñ09].

4 Data Treatment

The cup anemometer, vane and sonic data are compared with the lidar measurements at various heights, which were described in section 3. Furthermore, the lidar has 46 degrees offset compared with the meteorological mast, and this offset is taken into account in the lidar measurements. It means the North beam of the lidar has average 46 degrees offset with the geographical North, where the meteorological mast is located. Data are filtered to be able to carry out the comparison in identical conditions between the different instruments. On the other hand, filtering data causes a loss of the quality or detailed description of information the data set can provide.

4.1 Data Filtering

All of the measurements are on 10-min average wind speed and wind direction from Høvsøre. The database of Høvsøre measurements is used where 10-min average of 10 Hz measurement is stored. Data are filtered as described below.

Wind speed

Only mean wind speeds larger than 2 m/s are considered in this study. Very low and very high wind speeds are not investigated. In the aspect of wind energy applications, 2 m/s is chosen to be on the safe side considering conventional cut in wind speeds. Furthermore, if the wind speed is less than 2 m/s, it will probably not be able to move the vane.

Wind Direction

Easterly wind direction has to be analysed between 65 and 125 degrees (figure 4.1), since the wind is distributed much more in the interval of 60 and 165 degrees. At Høvsøre, the measurements are influenced by the characteristics of the surrounding land. It should take a narrower upwind sector that the average distance winds have to travel from the land to the mast is reduced. A narrower sector is not chosen because the number of available measurements are highly reduced [Flo13]. The wind direction is measured with vane, lidar and sonic at different heights. All directions at all heights are assumed to be in this sector.

Lidar Availability

Lidar availability is the percentage of data within an averaging period (10-min) in which the carrier to noise ratio is lower than a threshold value (-28 dB) [Peñ09].

Lidar CNR

The carrier to noise ratio is the ratio between the intensity of the received backscatter signal and the intensity of the measured level of noise, and the unit of CNR is in decibels (dB). The value of CNR is considered for more than -15 dB in this study.

  The number of data before filtering of all 4 steps that is explained above is 16181. The table 4.1 shows the number of data after each step that the measurements are retrieved. For instance, the amount of data has been reduced from 16181 to 13779 when the wind speed more than 2 m/s is considered. Then, they decrease to 6002 when the measurements are retrieved as the Easterly wind. Hence, the number of measurements are reduced to 1446 after all the filtering process are carried out and they are in the interval between November 2008 and April 2009. All of the instruments cover the same amount of data with the same time period.

4.2 Data Averaging

In this section the mean value of wind speed and wind direction will be computed. In this study data are based on 10-min wind speed and wind direction.
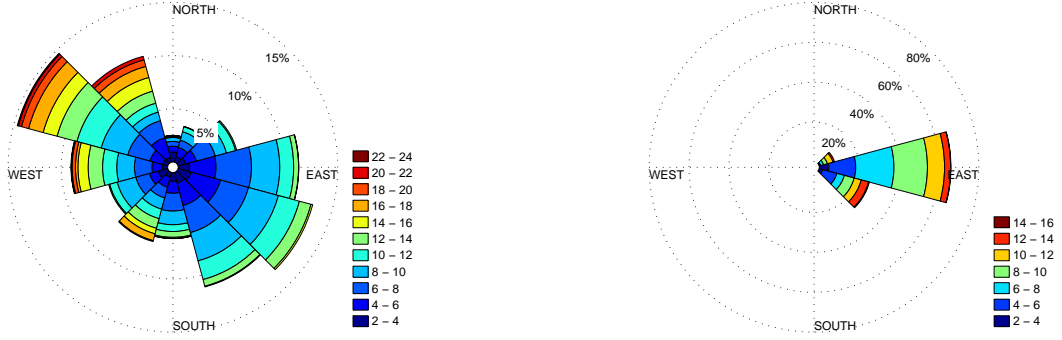
Figure 4.1: *Wind rose at Høvsøre site. It is observed at height 100 m between November 2008 and April 2009. Legend corresponds to wind speed in m/s.*

Table 4.1: Filtering of data

filter	Number of data points
before filtering	16181
Wind speed (> 2 m/s)	13779
Wind direction (Easterly)	6002
Wind direction ($65° < \theta < 125°$)	2011
lidar availability (100)	1807
CNR (> -15)	1446

The Wind Speed

When there is n measurements of wind speed, a mean wind speed, U is found as following

$$U = \frac{1}{n} \sum_{i=1}^{n} U_{z,i} \tag{4.1}$$

This method of calculating mean is called arthimetic mean. The standard deviation is computed to find the unsteadiness of the wind speed. In this study, the standard deviation of wind speed is calculated by Matlab function $std(U_i)$, and then the standard error of the mean is $\frac{std(U_i)}{\sqrt{n}}$.

The Wind Direction

The mean value of the wind direction, θ is calculated in different methods. Yamartino method is a suitable algorithm for computing the mean wind direction [Yam84]. The first step is to calculate the average values of $\sin(\theta)$ and $\cos(\theta)$ when n measurements of the wind direction are found. Thus, the mean value of $\sin(\theta)$ and $\cos(\theta)$ are computed as below

$$S_a = \frac{1}{n} \sum_{i=1}^{n} \sin(\theta_i) \tag{4.2}$$

$$C_a = \frac{1}{n} \sum_{i=1}^{n} \cos(\theta_i) \tag{4.3}$$

The mean wind direction is defining in the next step according to four-quadrant arctan(x, y) function

$$\theta_a = \arctan(C_a, S_a) \tag{4.4}$$

12

The right hand of Eq. (4.4) is expressed as $\mathrm{atan2}(C_a, S_a)$ in MATLAB codes, and in addition the unit of θ is in radian.

At last Yamartino defined standard deviation, σ_θ is computed as

$$E = \sqrt{1 - (S_a^2 + C_a^2)} \tag{4.5}$$

$$\sigma_\theta = \arcsin(E)(1 + \frac{2}{\sqrt{3}})(E^3). \tag{4.6}$$

The standard error of the mean can be calculated as $\frac{\sigma_\theta}{\sqrt{n}}$, where n is the number of measurements [Yam84]. In both cases, the uncertainty of measurements of the wind speed and wind direction are indicated using error bars.

In the following, it will be shown the difference in the calculation of the mean wind direction and the standard deviation based on the Yamartino method or the arthimetic mean. Three random directions, 10, 25 and 85 degrees in the first quadrant are chosen. The results of the mean value in both methods are illustrated in table 4.2. The result of Yamartino method shows that the mean wind direction is 1.1 degree larger than the arthimetic mean. The standard deviation result that is found from the Yamartino method is 2.1 degrees smaller than the other one. There is a significant difference between both methods. If the accurate method is not used, the predictions become less precise.

Table 4.2: The results of mean and standard deviation in two different methods

Methods	Mean value	Standard deviation
The Yamartino method	40	37.8
The normal method	38.9	39.9

5 Results

Linear regression analysis deals with modelling between two variables, y and x. In the present study, it is applied to the horizontal mean wind speed (mean wind direction) between lidar wind speed (wind direction) and reference wind speed (wind direction) [Coh+03]. The model is

$$y = kx + C \tag{5.1}$$

where y and x are lidar and reference wind speed (wind direction), and k and C define as regression slope and offset. Furthermore, there is a determination coefficient,R^2 to understand how the variables are correlated. In this study, the reference wind speed and wind direction are sonic anemometer and wind vane at height 10 m, respectively.

In this study, first, data filtering is carried out between cup and lidar wind speed at heights 60 m and 100 m, and different CNR are checked to find the value which has less signal noise and errors. Then, this process is checked between the vane and lidar wind directions. Figure 5.1 illustrates correlations for different CNR values at height 100 m between lidar-cup wind speeds and lidar-vane wind directions. In figure 5.2, when the value of CNR increases, the number of measurements decreases. Therefore, when figure 5.1 is complemented with figure 5.2, CNR value is chosen larger than -15 dB, in order to have sufficient number of measurements and high value of R^2.
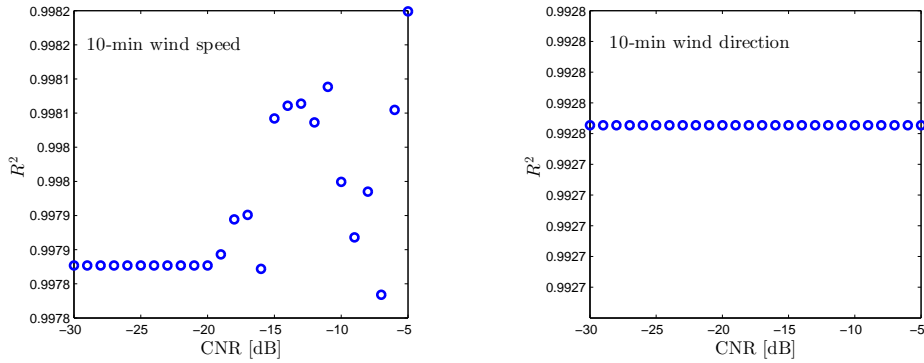
Figure 5.1: *Correlations for different CNR values between lidar and cup wind speeds at height 100 m (left panel), and between lidar and vane wind directions at height 100 m (right).*
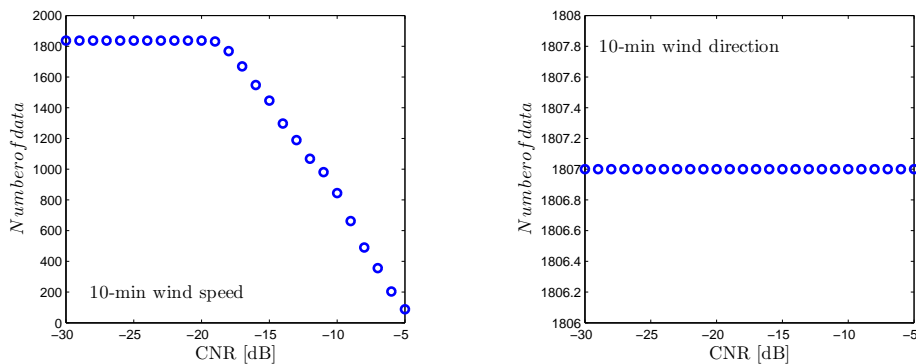
Figure 5.2: *The number of data for different CNR values between lidar and cup wind speeds at height 100 m (left panel), and between lidar and vane wind directions at height 100 m (right).*

Figure 5.3 shows a scatter plot of 10-min mean wind speed measured by the cup and sonic anemometers compared to that from the wind lidar at 100 m for the whole period. In this figure, there is good agreements between the wind speed from the lidar and the cup and sonic anemometers. It is seen in figure 5.3 that R^2 at both heights 100 m and 60 m are almost 0.99 which shows how well the wind speed distributions in these instruments are correlated. The lidar-cup wind speed comparison shows a slope very close to 1 but in the

lidar-sonic one is 0.97, i.e. 3 percent higher wind speeds than the sonic. This is because the sonic overestimates the wind speed. It is expected that the cup overestimates the wind speed contains a contribution from traverse turbulence fluctuations. It was explained in the previous section that the drawback of sonic anemometer is that it produces wind speed errors.
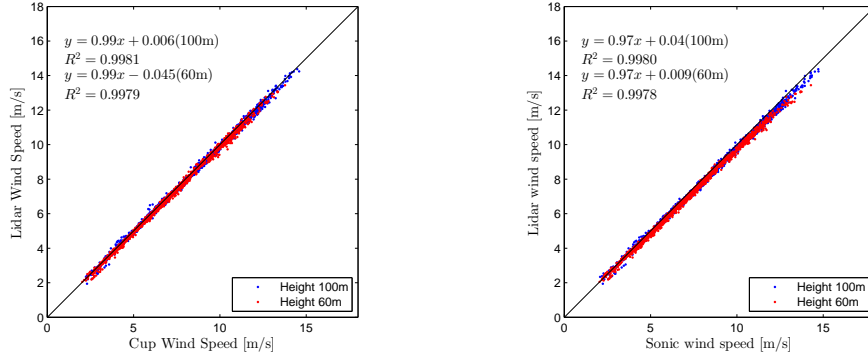
Figure 5.3: *Regression for mean wind speeds at heights 60 m (red dots) and 100 m (blue dots) in lidar, cup and sonic. At each height regression slope, offset and regression coefficient are calculated.*

The same process as explained above is used for linear regression analysis of the mean wind directions. In figure 5.4, R^2 indicates that there are good correlations between lidar, vane and sonic which is around 0.99. The lidar-vane wind direction comparison shows a slope very close to 1, whereas the slope in lidar-sonic is equal to 0.97. This difference in slope shows that the sonic overestimates the wind direction. There is a noticeable offset at height 100 m, for which sonic-lidar is +1.55 degrees, vane-lidar is -1.23 degrees and vane-sonic is -2.66 degrees. It means, for example, when sonic at height 100 m shows zero degree, lidar indicates 1.55 degrees. The offset of the wind direction does not necessarily mean that the wind lidar is wrong but that the sonic or vane are not perfectly aligned with the North or at least with the geographical North of the lidar.

5.1 The effect of stability

5.1.1 Vertical Wind Shear

Wind shear is the change in the wind speed with height in the atmosphere. In Eq. (2.2), $\frac{du}{dz}$ represents the wind shear influenced by the atmospheric stability.

The wind profile is considered according to its dependency on z/L in Eq. (2.5). The 10-min wind profile will be classified into different stability classes according to L. The wind characteristics within each stability classes are analysed. Table 5.1 indicates different ranges of stabilities, which are divided in very stable to very unstable according to the Obukhov length.

Table 5.1: Different stability classes according to Obukhov length [Peñ09]

Stability Class	Interval of Obukhov length L [m]
Very stable (vs)	$10 \leq L \leq 50$
Stable (s)	$150 \leq L \leq 200$
Near Stable (ns)	$200 \leq L \leq 500$
Neutral (n)	$500 \leq L, L \leq -500$
Near unstable (nu)	$-500 \leq L \leq -200$
Unstable (u)	$-200 \leq L \leq -100$
Very unstable (vu)	$-100 \leq L \leq -50$

It is seen in figure 5.5 how the mean value of U/u_* changes with logarithmic heights in different stability classes when lidar, cup and sonic are used. These measurements have been carried out at Høvsøre site and after filtering in the period between November 2008 and April 2009.
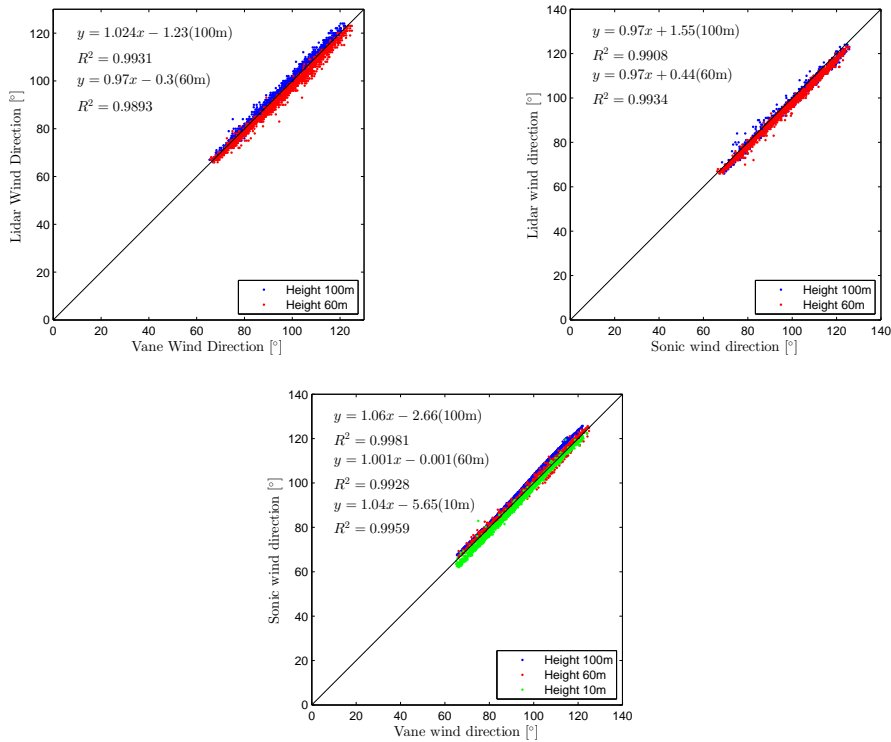
Figure 5.4: *Regression for mean wind direction at heights 60 m (red dots) and 100 m (blue dots) in lidar, vane and sonic, and at heights 10 m (green dots) between vane and sonic. Regression slope, offset and regression coefficient are calculated for each heights.*

In figure 5.5, as it is expected, the wind speed in stable condition increases with height with higher rate than all the other cases. This behaviour is explained by the strong wind shear in stable condition. On the other hand, there is a strong vertical motions of air in the unstable condition which gives lower increase of wind speed in comparison with all other conditions. Furthermore, the wind speed observations follow a concave or convex shape as expected in the stability cases or a straight line in the case of neutral conditions.

Figure 5.6 illustrates the comparison of cup anemometer, sonic and lidar wind speed profile. It is seen that each class of stability for these three instruments overlaps on each other, which shows all three instruments have had the same results in measurements of wind speed with heights. There is a good agreement between the wind speed of all three instruments. In some heights, there are small differences in wind speed with different instruments, which the combination between slope and offset in figure 5.3 illustrate.

5.1.2 Wind Turning

A change in a wind direction with height is called a wind turning. When the wind turning in the Northern hemisphere is clockwise, i.e. from the North to the Northwest, it is known as a wind veer. Whereas a backing wind is the wind turns counter clockwise in the Northern hemisphere [Hab13].

In the following, the wind direction profiles of lidar, vane and sonic are analysed in various stability classes (figure 5.7). The difference in the wind directions of all three instruments are presented with the reference vane at height 10 m. It is expected that the wind directions vary with heights close to zero in very unstable and unstable conditions due to the strong vertical motions. By contrast, the change in the wind directions in very stable and stable cases are significant, because of the strong wind shear. It is clearly seen in figure 5.7 that very unstable wind turning has similar behaviour to that in near stable condition. This unexpected behaviour can be explained by the following reasons. First, the values of heat flux have been very low in very unstable and unstable conditions, where were only 19 percent of the data have had high heat fluxes. However, the friction velocities change reasonably in proportion to the wind speed in those two conditions. Second, error bars (figures 5.8, 5.9 and 5.10) in all three instruments show that very stable, near unstable, unstable and very unstable cases have had errors around 4 times bigger than stable, near stable and neutral conditions. The third
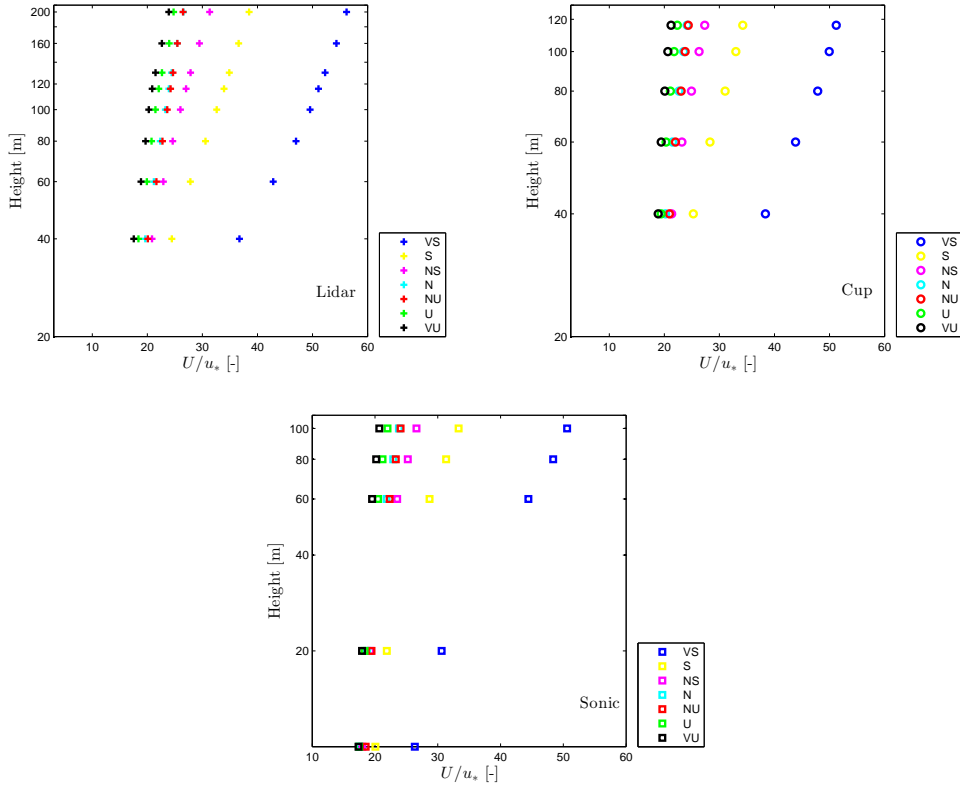
Figure 5.5: *Wind profile of lidar (top left), cup (top right) and sonic (on the bottom) in different stability classes. Legend information is given in Table 5.1.*

reason is the number of measurements in those four cases have been smaller than 40 which is considered as low.

The other reason which may affect the wind turning is baroclinity but is not considered in this study. Floors explained that baroclinicity has a large effect on the wind veer in the boundary layer because the forcing is changing with height. He mentioned in his thesis report that the effect of baroclinicity on the wind profile in the boundary layer was recognized a long time ago and studying its influence is often based on large-eddy simulation data [Flo13]. In the case of very unstable and unstable conditions, there are two days (November 29 of 2008 and April 15 of 2009) that the change in the wind directions has not been similar as the other data. It means that the wind direction, instead of changing around zero degree, has a higher variation with different shape. Around two third of the measurements in very unstable condition and about half of data in unstable case follow this behaviour.

Another unexpected behaviour is related to the shape of the sonic wind direction profile. Each stability class does not follow its concave or convex shape or a straight line. This behaviour shows that the sonic anemometers at different heights are probably not mounted exactly to the North, and they are installed with an offset.

Figure 5.8, 5.9 and 5.10 show the error bars of lidar, vane and sonic wind turning, respectively. In all three instruments, stable, near stable and neutral conditions have small variability around 0.8, 0.6 and 0.6 degrees. By contrast, near unstable, unstable and very unstable error bars are approximately changed 2.6, 2.5 and 2.4 degrees. These variabilities indicate low certain behaviour of near unstable, unstable and very unstable observations.
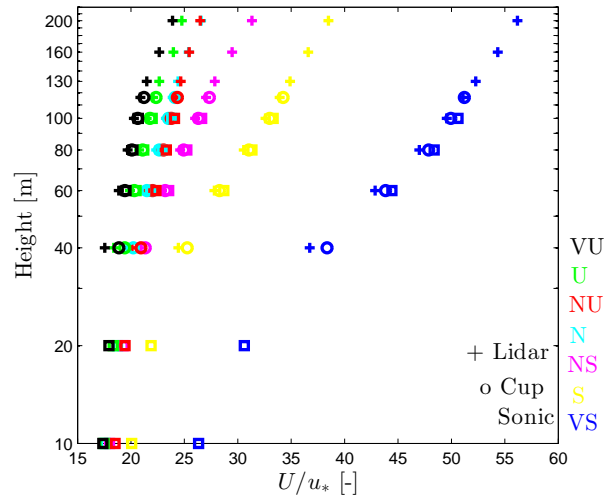
Figure 5.6: *Comparison of lidar, cup and sonic wind profile at different stability classes and heights. Lidar shows with plus sign, sonic with square and cup with circle. Different colors are related to different stability.*
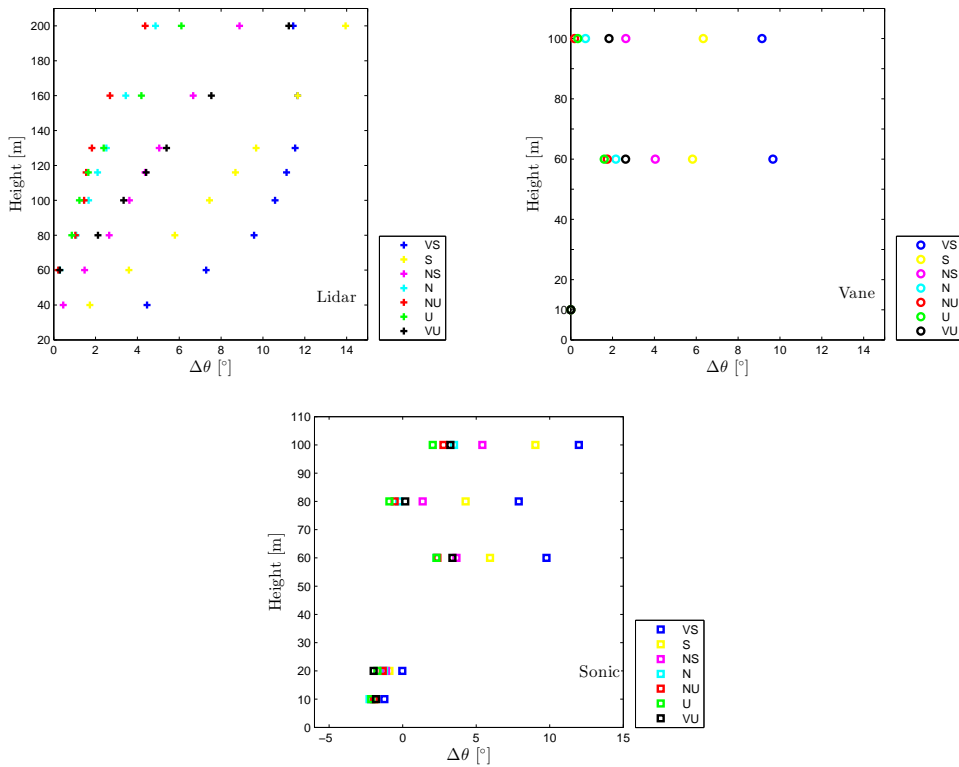
Figure 5.7: *The wind direction changes with heights in various stability classes in lidar (top left), vane (top right) and sonic (on the bottom). $\Delta\theta$ indicates the difference in wind direction in each instrument from reference vane wind direction at height 10 m.*
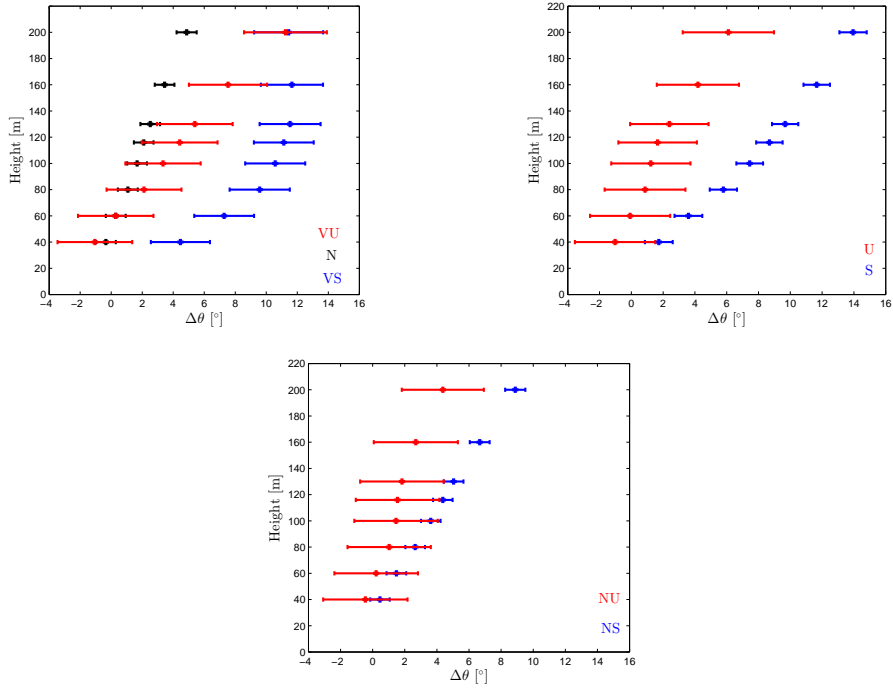
Figure 5.8: *Error bers of the wind turning behaviour in lidar in seven stability classes. The top (left) plot consists of very stable, neutral and very unstable wind. Stable and unstable wind error bars are shown on the top (right). Near stable and near unstable are on the bottom of the figure.*
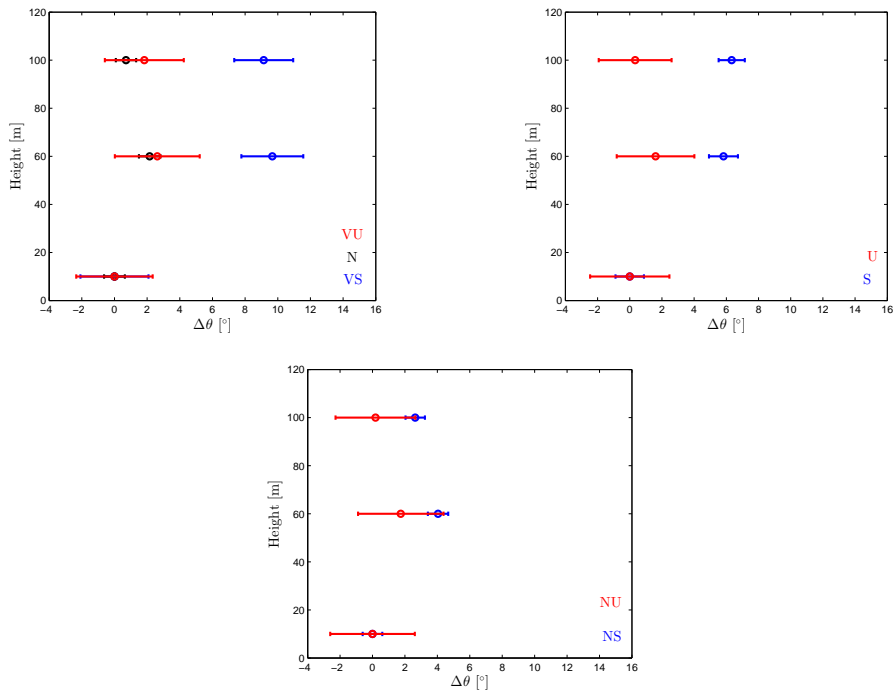
Figure 5.9: *Error bars of the wind turning behaviour in vane in seven stability classes. The top (left) plot consists of very stable, neutral and very unstable wind. Stable and unstable wind error bar is shown on the top (right). Near stable and near unstable are on the bottom of the figure.*
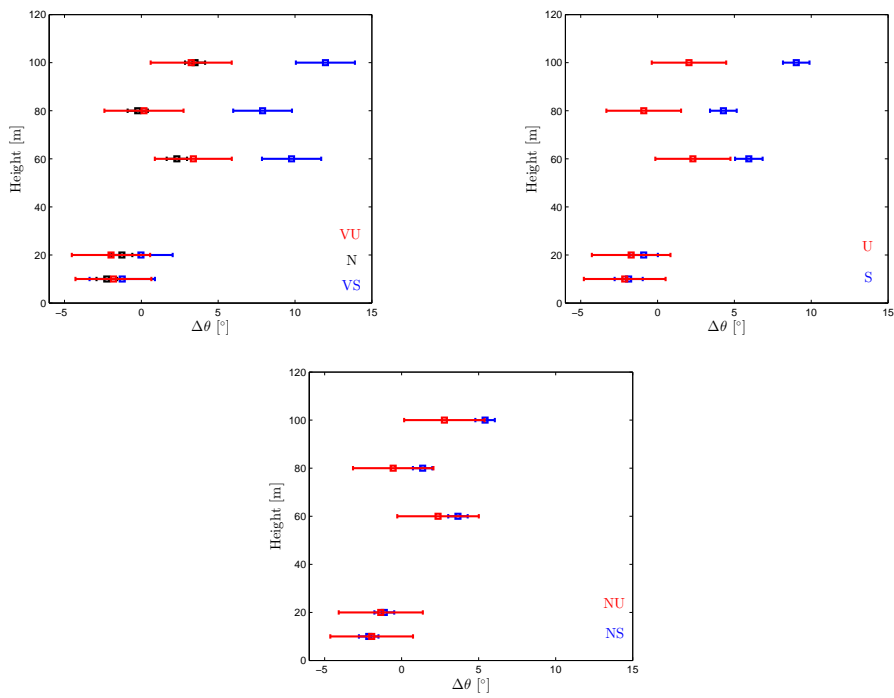
Figure 5.10: *Error bars of the wind turning behaviour in sonic in seven stability classes. The top (left) plot consists of very stable, neutral and very unstable wind. Stable and unstable wind error bars are shown one the top (right). Near stable and near unstable are on the bottom of the figure.*

In figure 5.11, the change in lidar, vane and sonic wind directions have been compared. Figure 5.4 illustrates that the behaviour of the difference between those three instruments at height 60 m and 100 m are related to their offsets and slopes. For example, at height 100 m in very stable case, lidar measurements are smaller than sonic measurements with difference of less than two degrees. It has to be noticed that figure 5.4 compares wind direction between different instruments, but in figure 5.11 the difference in wind direction of each instrument with the reference wind direction of vane at height 10 m has been analysed. Thus, the value of offset at 10 m vane has to be subtracted to the offset value in sonic, vane and lidar at height, i.e. 100 m. Then the sign of offset may change and explains the lidar, vane and sonic data in figure 5.11.
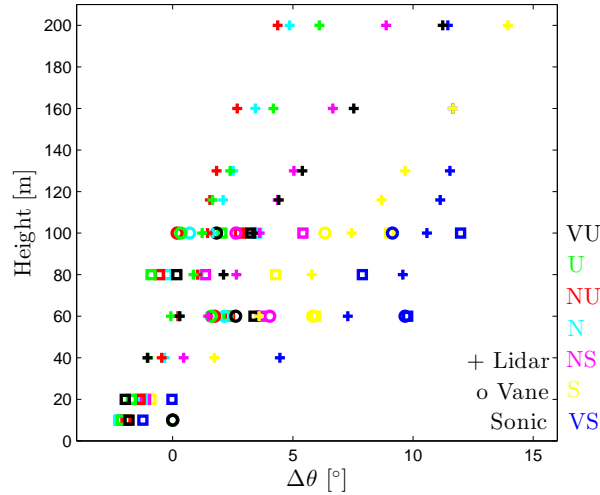
Figure 5.11: *The comparison of lidar, vane and sonic wind turning at different stabilities and heights. $\Delta\theta$ indicates the difference in wind direction in each instrument from reference vane wind direction at height 10 m. Lidar shows with plus sign, sonic with square and vane with circle. Different colors are related to different stability classes.*

5.2 Monthly Evolution

5.2.1 Vertical Wind Shear

Figure 5.12 (left panel) compares the changes in wind speed of lidar, cup and sonic between height 100 m and sonic reference at height 10 m. In figure 5.12, the change in wind speed is analysed, whereas in figure 5.3, the wind speed is considered in the observations. Therefore, the wind speed has to be subtracted between two heights to find a correct offset value and sign. When this process is carried out, the measurements by three instruments are concluded as it is shown in figure 5.12.

It is found that the wind shear has different characteristics in different months. According to the figure, the increasing rate in the wind shear is seen from November to January and then the similar behaviour in January, February and March. The snow covers the surface during the winter at Høvsøre, and it makes the surface becomes colder than the air. Hence, this explanation justifies the behaviour of the wind from November to March as the weather start becoming cold from November. The value of wind shear reduces from March to April, and that is probably because of the changing weather. In November and April, the amount of data is very low, and the results can be uncertain.

The figure 5.12 (right) shows the difference in wind speed of cup and sonic with the sonic reference wind speed at height 10 m where there are no lidar measurements. The strong wind shear occurs between July and September that was the warmest period of the year. In June, the weather is starting to be warm. In the year 2009, July was the hottest month and September had 24 consecutive warm days with temperature higher than average [DN09]. This unexpected behaviour in these three months is explained by lacking of data between time 16:00 and 20:00 in July, and from 11:00 to 16:00 in August. The fact is that the hours around noon are missing and hence there may be a convective period. There are no measurements around 5 hours during the day which unstable condition is dominating. Therefore, it is reasonable that the results show the high wind shear in July and August.

The error bar in figure 5.12 (left) shows that data reliability on November and April is smaller than the other months, due to high variabilities in November and April. The same explanation is valid for July, August and September (Figure 5.12, right).
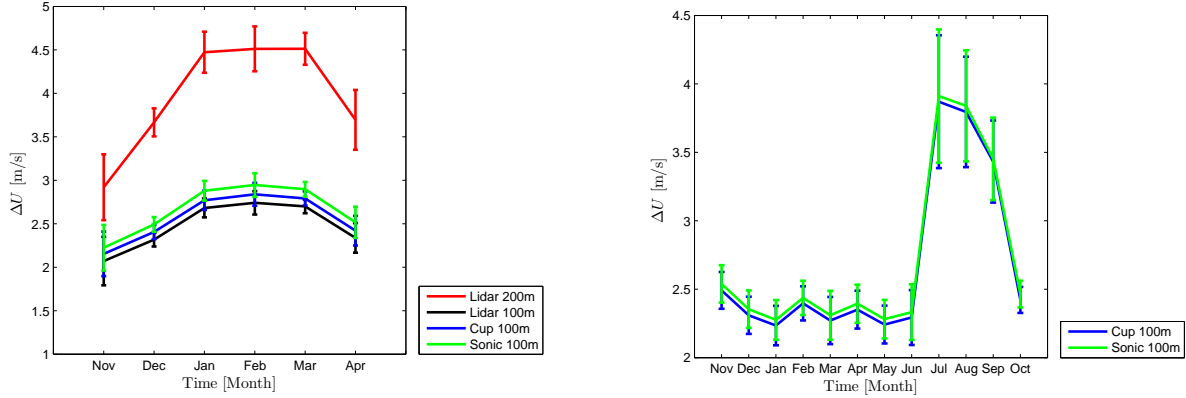
Figure 5.12: *Wind shear in lidar, cup and sonic from December 2008 to April 2009 (left). ΔU indicates the difference in wind speed of each instrument from reference sonic wind speed at height 10 m. The figure (right) is sonic and cup wind shear without considering lidar during 12 months (from November 2008 to October 2009). Error bars of both cases are shown in the figure.*

5.2.2 Wind Turning

Figure 5.13(left) compares the wind turning in lidar, vane and sonic which have been measuring the change in wind direction between heights 100 m and the reference vane at 10 m. Besides, the difference in wind direction is indicated in the same plot for lidar at 200 m. As it is clarified in the previous section, figure 5.4 shows the offset in wind direction for lidar, vane and sonic, while figure 5.13 shows the difference in wind direction. The offset value is found according to the difference in wind direction, the offset sign may change. This is because the vane, sonic and lidar measurements are located differently at the same height in figure 5.13.
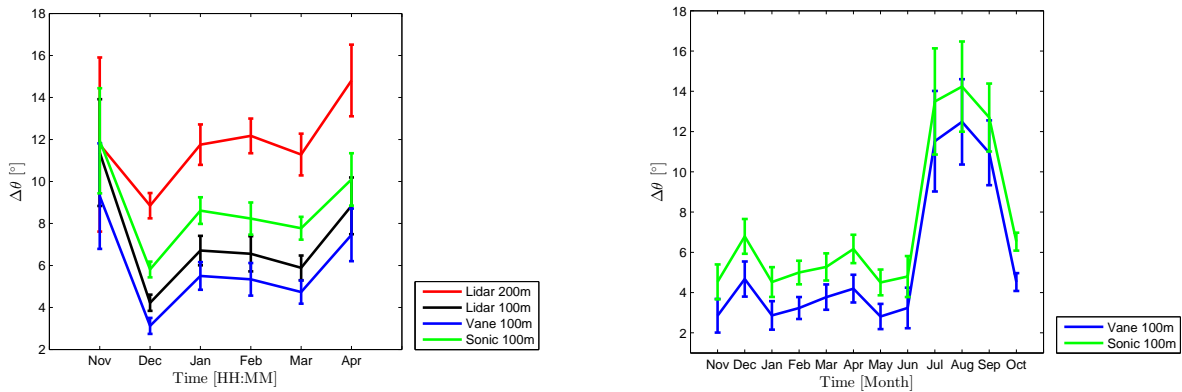
Figure 5.13: *Wind turning behaviour in lidar, vane and sonic from December 2008 to April 2009 (left). $\Delta\theta$ indicates the difference in wind direction in each instrument from reference vane wind direction at height 10 m. The figure (right) is sonic and vane wind turning without considering lidar during 12 months (from November 2008 to October 2009). Error bars of both cases are shown in the figure.*

There is a significant reduction in $\Delta\theta$ from November to December in figure 5.13 (left). It is expected that the strong vertical motion occurred in November, because of the wind shear behaviour in figure 5.12. This distinction probably happens, due to the different choice of reference. The other reason is related to errors in November and April that are big compare to other months. Furthermore, as explained before, two days in

November and April wind behaves differently which has an effect on the wind turning in very unstable and unstable cases and they behave similar to stable winds. Figure 5.14 shows the number of measurements that exist in every month and based on different stability classes. The fewest amount of data is in November and then April. In November, there is only three days measurements.

The variation of the wind turning in January, February and March is small. It means that the wind turning has had a similar behaviour in these three months.
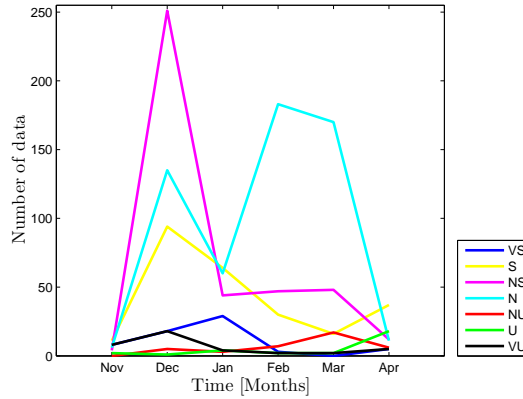
Figure 5.14: *The amount of data that is classified by months and each stability classes. Different colors are related to each stability conditions.*

Figure 5.13 (right) shows the change in the wind direction between November 2008 and October 2009 when lidar is not considered in the measurements. In this comparison, only vane and sonic are investigated to observe how the wind turning acts in the other months. The wind turning is assumed between the height 100 m of the vane and sonic and the reference vane at height 10 m. From June the variation in wind direction goes up and then there is a sharp reduction in October. As it is explained in subsection 5.2.1, in July and August the measurements do not exist during 5 hours in a day. It shows that data is related much more to those times that there is stable condition. Hence, the high change in the wind turning from June to July, and then the sharp reduction in October is related to low amount of data during the day (unstable condition). In conclusion, the wind shear characteristics are in the agreement with the wind turning in the duration of one year.

Error bar in figure 5.13 (right) illustrates the measurements in July, August and September have been more uncertain due to fewer measurements and high variabilities in these months.

5.3 Daily Evolution

5.3.1 Vertical Wind Shear

The difference in wind speed during average of 24 hours of the whole 6 months is shown in figure 5.15. The purpose of expressing average 24 hours in the whole period or different months is that the time is divided in to 24 hours with the interval of one hour. For instance, one of the period is from time 00:00 to 1:00 (00:00 is equal to time 24:00) and then all of the measurements in a month, i.e. December, or the whole duration in this one hour are collected and the mean values of them are calculated. In addition, the changes in the wind speeds are considered between height 100 m and reference sonic 10 m, and wind lidar at 200 m is also checked. Night time is supposed to be from time 18:00 to 6:00, and a day is defined from 6:00 to 18:00.

In figure 5.15, there is a strong wind shear at night compared to the day time. Therefore, the wind is unstable during the day and has stable behaviour at night, in general. The maximum fluctuation of wind shear is around time 21:00, whereas the lowest wind shear happens at noon as expected. The error bars of daily wind shear are illustrated in figure 5.15, which are in the same ranges of uncertainty, and the variability of them is small.

Figure 5.16 illustrates the average of wind shear every one hour in the whole 24 hours in different months. November is not included in the figure because the number of measurements is very low and the plot does not make sense. The highest change in wind speed(stable condition) has occurred during time 9:00 to 13:00 in
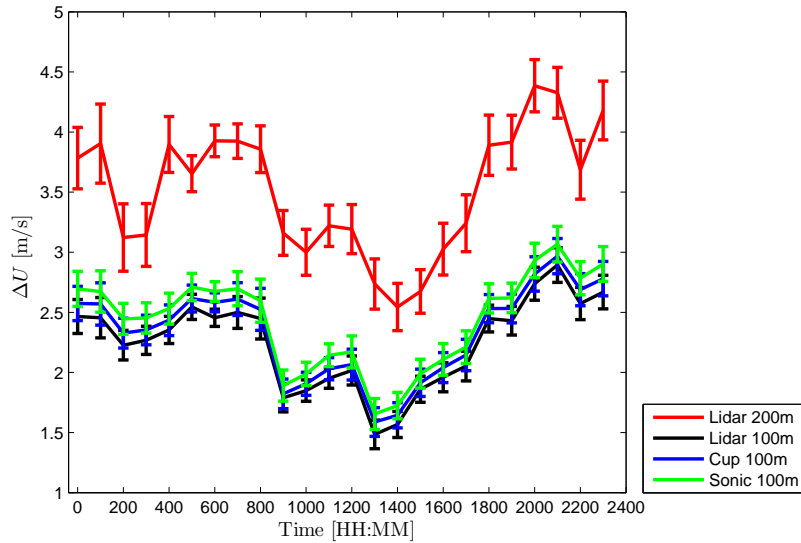
Figure 5.15: *Average diurnal comparison of lidar, cup and sonic wind shear from November 2008 to April 2009. ΔU indicates the difference in wind speed of each instrument from reference sonic wind speed at height 10 m. Error bars of the diurnal behaviour of three instruments are shown in this figure.*

December. Between time 23:00 and 8:00, ΔU has lower value than the other 24 hours, and besides, the strong wind shear during the day in February is obvious. At night, the surface is colder than the air and it is expected to be stable condition, but in December it is the opposite. This unexpected behaviour is explained by existing snow in the winter at Høvsøre site, that during the day the surface is colder than the air. In January, the stable condition is much more common than unstable, especially at night.

Furthermore, the wind speed has not changed significantly in March 2009, except from time 8:00 to 12:00 and 18:00 to 22:00 when the wind shear was reduced. It means that unstable condition is distributed in the morning and at night. Figure 5.16 (on the bottom) shows the change in wind speed in April. It is seen that there are not any data in some hours of a day, because the measurements do not exist on those times after filtering.

5.3.2 Wind Turning

Figure 5.17 indicates average diurnal wind turning. During a period of about 4 hours in the morning, $\Delta\theta$ has been close to zero that describes unstable condition. In general, the difference in wind direction during the day has been less than during the night and it is in agreement with expectations. The diurnal wind shear and the wind turning in the period of six months are proportional to each other, except between time 22:00 and 2:00 when they behaved in opposite.

It is seen in figure 5.18 how the wind direction changes during the average 24 hours in five different months. When the change in the wind direction is close to zero, it means there is an unstable wind which usually happened during the day when the surface is warmer than the air and the heat flux is high.

In December after 18:00, the wind turning has a reduction rate, which shows unstable condition occurred during the night. The wind direction has a fluctuation rate between 6:00 and 18:00, but it increased in general. This unexpected behaviour is justified as explained for the wind shear in the previous subsection. The most unstable wind behaviour happens in the morning in January. The wind turning has had much more fluctuation during the day in February, and besides it has been generally in stable condition at night.

In March, as it is expected, the wind direction difference has been generally small during the day, especially between 9:00 and 16.00. This means that there is unstable wind during the day and vice versa at night. As it was described in the wind shear subsection, there are no measurements in some hours in April, which explains that its diurnal behaviour is not precise. Wind lidar at 200 m has almost the same pattern as the other instruments in different months, but with higher uncertainty.
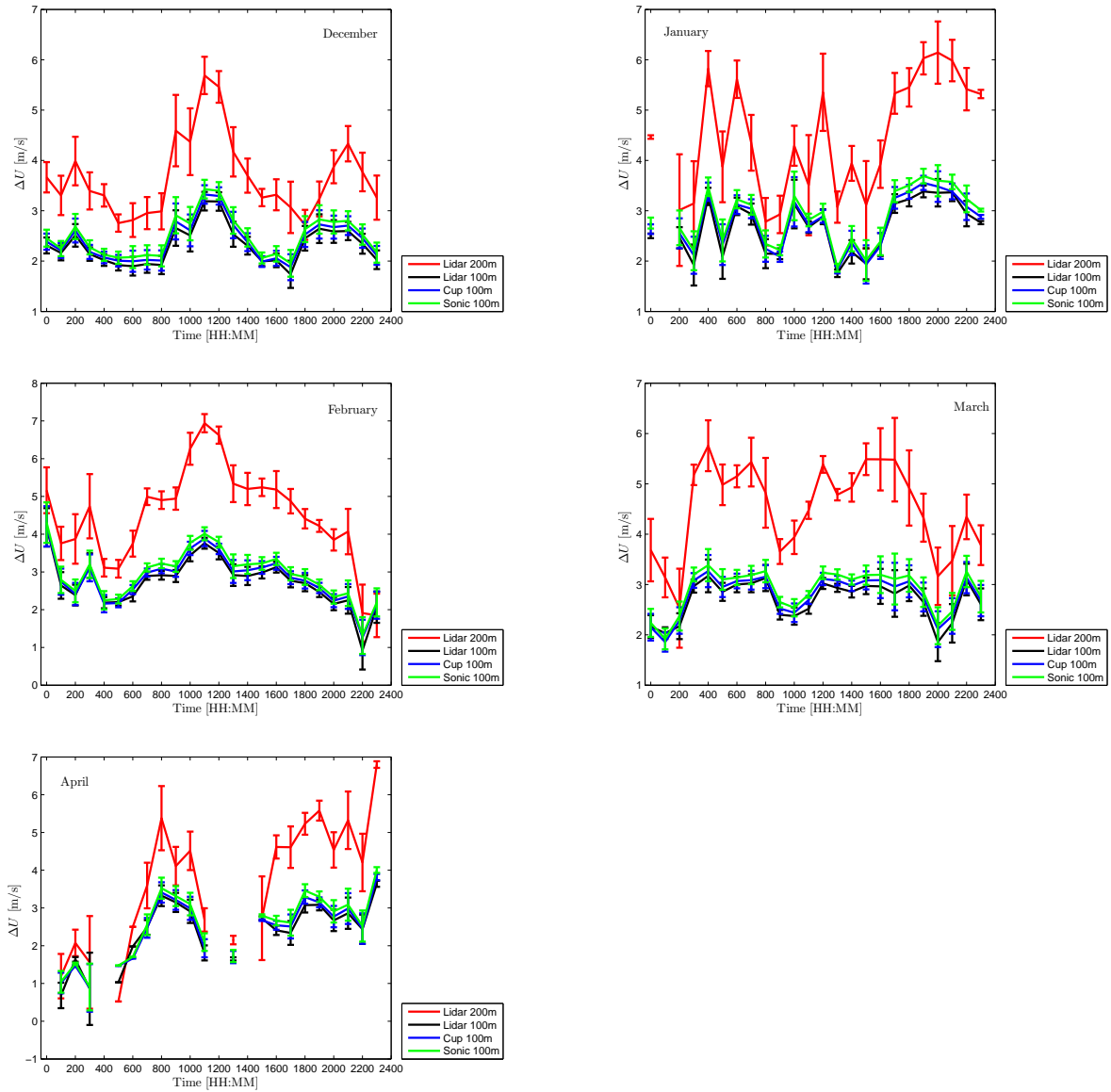
Figure 5.16: *Lidar, cup and sonic wind shear behaviour on December, January, February, March and April during average 24 hours. ΔU indicates the difference in wind speed of each instrument from reference sonic wind speed at height 10 m. Error bars of wind shear behaviour in lidar, cup and sonic are shown in the figure.*
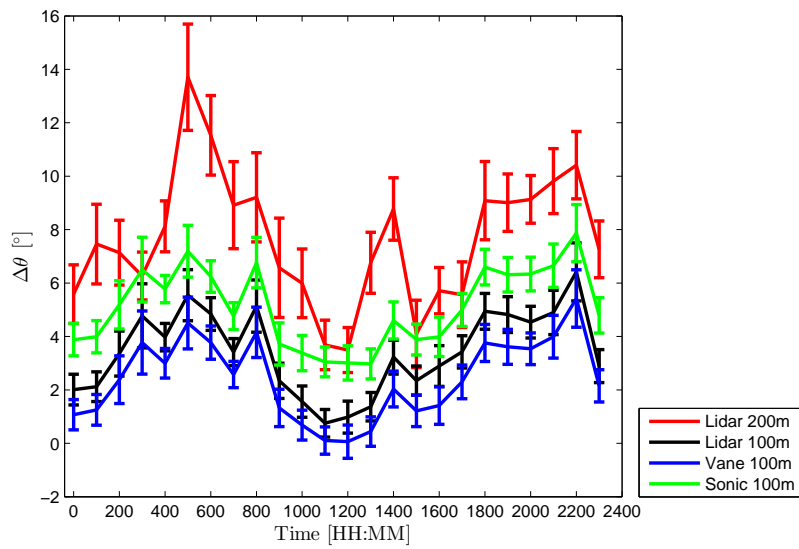
Figure 5.17: *Average diurnal comparison of lidar, vane and sonic wind turning from November 2008 to April 2009. Δθ indicates the difference in wind direction in each instrument from reference vane wind direction at height 10 m. Error bars of the diurnal behaviour of three instruments are shown in this figure.*
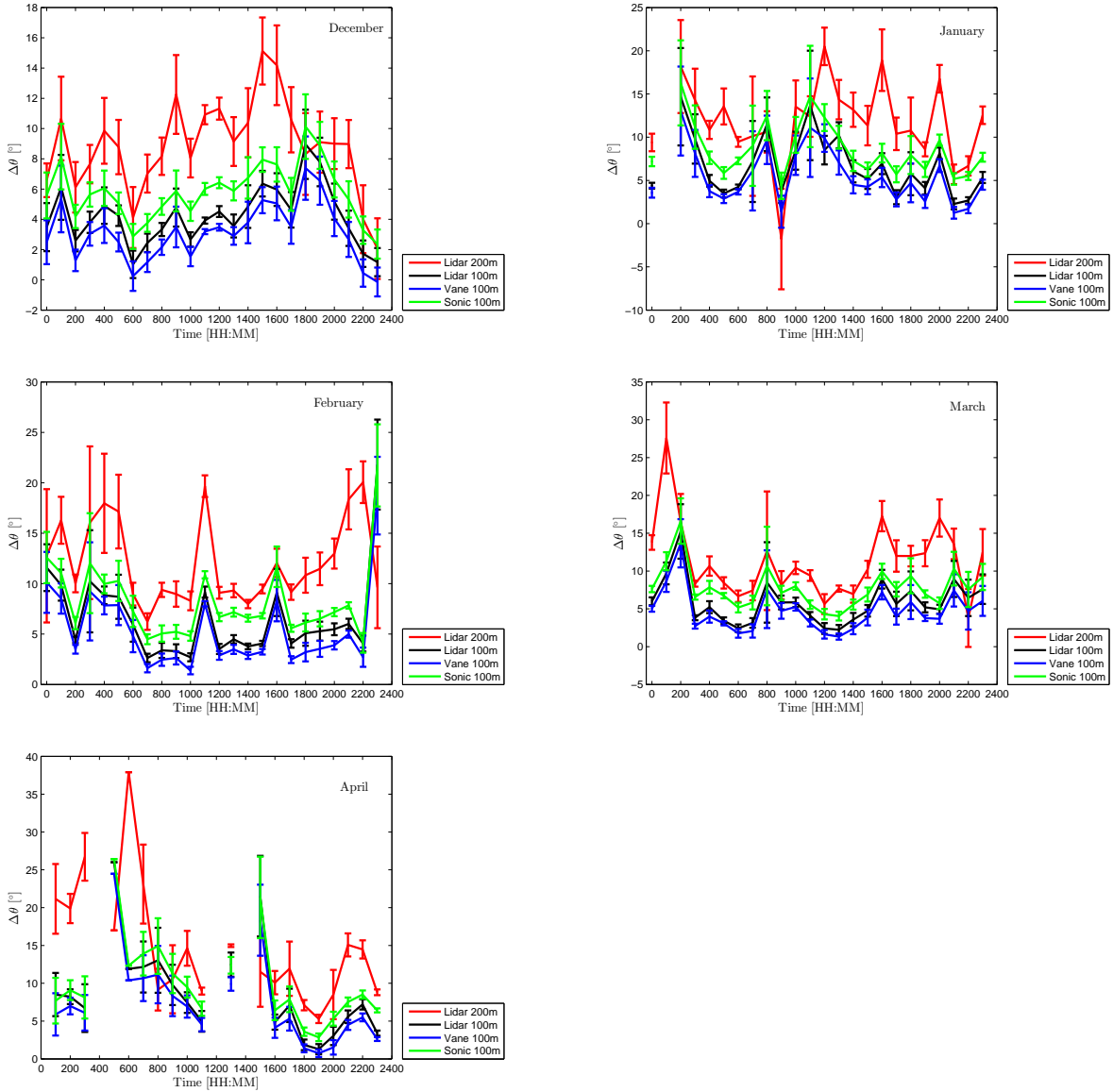
Figure 5.18: *Lidar, vane and sonic wind turning behaviour on December, January, February, March and April during average 24 hours.* $\Delta\theta$ *indicates the difference in wind direction in each instrument from reference vane wind direction at height 10 m. Error bars in mean diurnal wind turning behaviour in lidar, vane and sonic are shown in this figure.*

5.4 Non-dimensionalization

Non-dimentionalization is often employed to reduce the number of parameters and to better reveal the characteristics of a system. In figure 5.11 and 5.6, it is seen in the wind speed and wind direction profile that each stability conditions has different slopes. In this section, the case is to merge the 7 stability classes with 7 slopes, and find one slope. In the following, it will be shown whether it is possible to find the equation to calculate the wind speed and wind direction at each height, specially, at those heights for which the instruments are not mounted.

5.4.1 Vertical Wind Shear

The wind profile of different stability classes are plotted in subsection 5.1.1. Each of seven stability classes had different wind shear characteristics. Every instrument measures the wind speed and wind direction at various heights. As the ABL is a mixture of all kinds of stability cases, each of these ones has different boundary layer heights (z_i). For example, stable layer is in the lower height more common than neutral or unstable cases. In the scaling height, z/z_i, different values for z_i in each stability classes are checked until all of them collapsed in one line. This process is carried out for U/u_* versus logarithmic value of z/z_i for different instruments, which are lidar, cup and sonic. Table 5.2 shows the values of boundary layer heights related to each stability class at Høvsøre site.

Table 5.2: Value of z_i for different stability classes after non-dimensionalization.

Different stability classes	z_i [m]
Very stable	50
Stable	200
Near stable	460
Neutral	750
Near unstable	770
Unstable	1100
Very unstable	1400

Figure 5.19 collects the non-dimensionalized velocity profiles under different stability conditions and measured with all three instruments. As can be seen, the non-dimensionalized velocity profile is shared by various stability conditions. All of these three instruments with their collapsed data are compared in a figure 5.20. It is seen all of them are approximately in the same line which is a polynomial degree 2.

The relation between z/z_i and U/u_* is found according to the following

$$\frac{U}{u_*} = 1.41(\ln\frac{z}{z_i})^2 + 11.2(\ln\frac{z}{z_i}) + 40.35 \tag{5.2}$$

$$\frac{U}{u_*} = 28/k[(\ln\frac{z}{z_i}) + 7.95(\ln\frac{z}{z_i})^2 + 2.5] \tag{5.3}$$

where $k = 0.4$ is von Kármán constant, and z is the height above the ground. U and u_* are the horizontal wind speed and the friction velocity, respectively. Eq. (5.3) is valid at Høvsøre site.

In figure 5.21, blue dots illustrate that lidar, cup and sonic data collapse on to one line. The red line is the fitted line related to these data, and it is expressed in Eq. (5.3).

5.4.2 Wind Turning

The values of z_i that are found for the wind speed in seven stability classes in subsection 5.5.1 (Table 5.2) have been used for the wind direction profile. The turning of the winds in different stability conditions have not collapsed in one line, however this non-dimensionalization occurred for wind speed profile.

Figure 5.22 illustrates non-dimensionalization of lidar, vane and sonic wind turning. Very stable measurements have larger slope than other stability conditions. Then, $\frac{z}{z_i}$ is considered between zero and 1 to observe whether other stability conditions are collapsed or not. It is seen that stable, near stable, neutral and near unstable
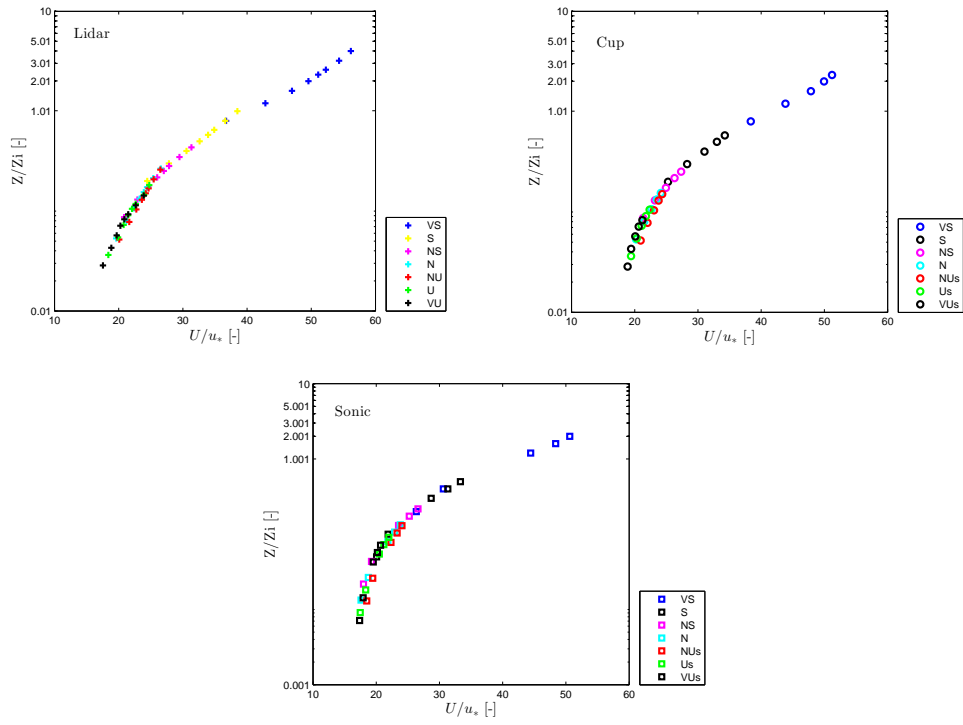
Figure 5.19: *Collapsing of lidar, cup and sonic wind speed variation in different stability classes.*

measurements in lidar are close to collapse but not in very unstable and unstable. As it is explained before, very unstable and unstable wind turnings have not shown reasonable characteristics in wind direction profile. Once again in vane and sonic, the shape of profile has not been as expected. Therefore, these unexpected behaviours may be affected non-dimensionalized data in lidar, vane and sonic.
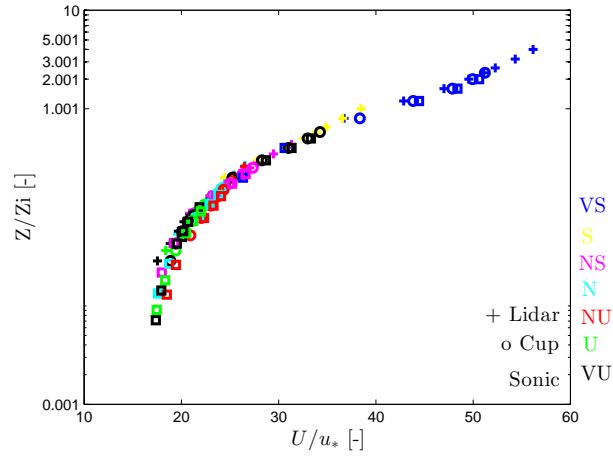
Figure 5.20: *the combonation of the collapsed data of lidar, cup and sonic wind speed variation in different stability classes from November 2008 to April 2009. z/z_i is logarithmic*
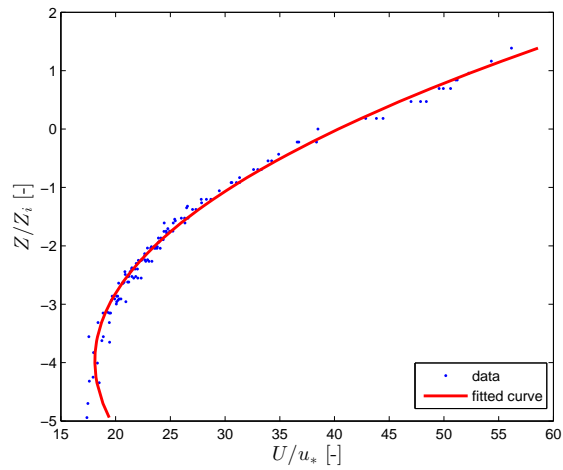
Figure 5.21: *Fitting of non-dimensionalized data in lidar, cup and sonic.*
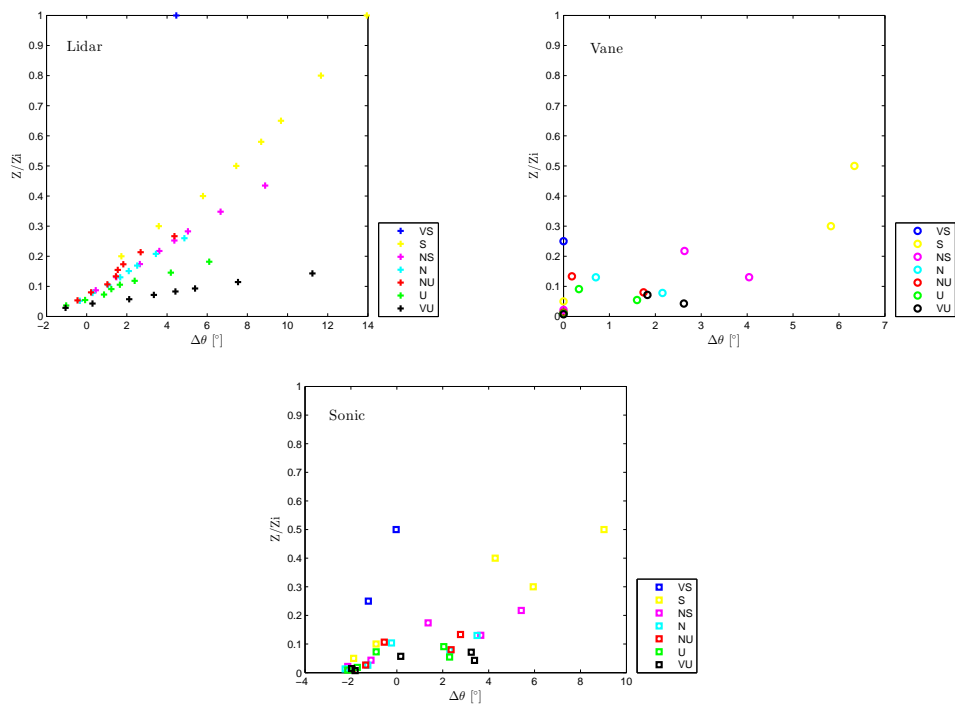
Figure 5.22: *Non-dimensionalization of lidar, vane and sonic wind turning variation in different stability classes.* $\Delta\theta$ *indicates the difference in wind direction in each instrument from reference vane wind direction at height 10 m.*

6 Discussion

In this section the results of the wind shear and the turning of the wind are analysed. At the end, the comparison between the wind shear and wind turning are carried out in more detail.

Vertical wind shear and wind turning

The wind speed profiles measured by lidar, cup and sonic at heights below 100 m behave as expected in the surface layer. The slope of the wind speed profile matches accurately to different stability classes. Furthermore, the wind speed observations by lidar behave as expected between heights 100 m and 200 m. They follow the shape of the stability conditions in agreement with their shape in the surface layer. Therefore, the wind speed observed by lidar shows the same accuracy as the cup/sonic wind speed measurements.

The wind turning observations by lidar, vane and sonic do not behave as expected in the surface layer. Very unstable wind shows a behaviour similar to near stable condition in all three instruments. In lidar, the wind direction profile follows the shape in agreement with different stability cases, except in very stable and very unstable conditions. As expected in very stable condition, the change of $\Delta\theta$ with height approaches to an asymptote at heights above 100 m. An unexpected behaviour is that $\Delta\theta$ in very unstable and unstable conditions change highly, instead of changing around zero degree. Three reasons could explain these unexpected results. First, the heat fluxes are very low in very unstable and unstable conditions. Only a small fraction of data shows the convective characteristics. Another explanation could be that the number of measurements are very low in very unstable and unstable cases. It might have an effect on the uncertainty of measurements. Finally, one day in November and April the change in wind direction in very unstable and unstable conditions has been similar to near stable case. It means that as the heights increase, the slope of the wind turning behaviours reduce instead of increase.

In vane and sonic, the shape (concave, convex or straight line) of the wind direction profile does not match to seven stability classes in the surface layer. The reason might be that the vane and sonic at all heights are not exactly mounted to the North, and the offset at various heights is different.

The comparison between the Vertical wind shear and wind turning

The wind shear and the wind turning from November 2008 to October 2009 is analysed between cup, vane and sonic without considering lidar. The comparisons between the measurements of cup-sonic and vane-sonic show that the wind shear and the wind turning from March to April had an increase rate. Since the measurements exist in all times of 24 hours during both months, they are much more reliable than the measurements in figure 5.12 and 5.13 (with lidar observations). Hence, it is predicted that in figure 5.12 and 5.13 (left panel) the wind shear and the wind turning should be in an increasing rate from March to April.

The average diurnal wind shear from November to April has been in agreement with the wind turning, however, they have not behaved in the same way in some hours of the whole 24 hours, i.e. from 10:00 to 12:00, and 2:00 to 4:00. This behaviour can be seen in the mean diurnal wind shear and wind turning of each month. The explanation for this result is that the wind turning in very unstable and unstable cases has a behaviour similar to near stable. Hence, those times which show high $\Delta\theta$, they can be stable or unstable wind. The wind turning and wind shear might be in agreement but because of very unstable and unstable behaviours, it seems they are in contradiction.

Monthly evolution of the wind shear and wind turning shows that the wind shear and the wind turning are in agreement from December to March, but in November and April they behave oppositely. The reason might be related to lack of measurements at some times of 24 hours. In April, there are not any data after filtering between time 11:00 and 15:00, and from 3:00 to 4:00. It seems that the results have to show high wind shear and wind turning. In November, there is low amount of data, which is distributed during night, and that is the reason $\Delta\theta$ in November is higher than the other months.

The present study has not investigated the physical effect on wind to figure out exactly the reason of unexpected behaviour of the wind turning profile. Thus, it is recommended to further study this field and find a further precise justification. Furthermore, the contradiction between wind turning and wind shear in some periods of time makes the need of more research in the turning of the wind in the future.

7 Conclusion

The wind speed and wind direction profile in the ABL have been measured by combining cup, sonic and vane at meteorological mast with lidar observations overland at Høvsøre, Denmark. This study is carried out by averaging the 10-min wind speed and wind direction measurements in wide range of atmospheric stability conditions from November 2008 to April 2009.

The easterly wind speed measurements within a flat and homogeneous sector show that the various instruments have been in a good agreement in different stability classes. By contrast, the changes in the wind direction measurements behave unexpected in very unstable conditions in all three instruments.

The mean wind shear during the average 24 hours from November 2008 to April 2009 shows high wind shear during night and few hours early in the morning. Therefore, the average diurnal behaviour of wind shear in the whole period has been in agreement with the expectation. The wind turning shows the same result during the whole period. The average daily wind shear are compared to the mean diurnal wind turning in the whole period of measurements. It shows the daily wind shear to be in agreement to the diurnal wind turning.

The significant difference of the mean diurnal wind shear of each month is related to the period of 8:00 to 14:00, and 18:00 to 23:00. Between 8:00 and 14:00, the wind shear behaves strongly in December and February, whereas in March it has opposite behaviour. During time 18:00 and 23:00 in December, the change in the wind speed is high, but it behaves vice versa in February and March. The rest of 24 hours in December, February and March, the behaviour of wind shear has been approximately constant. The average daily wind turning of each month indicates that the wind turning fluctuations have been high. In January and February, $\Delta\theta$ has high value around noon, whereas in March it shows opposite behaviour. In December, $\Delta\theta$ varies during different times and it shows stable behaviour after 12:00.

The mean wind shear of six months has behaved as in the same way as the mean wind turning, except in November and April. There is lack of data in some hours of the day in these two months. Thus, the wind shear is in agreement with the wind turning during the six months. The comparison between sonic and cup wind shear and wind turning are accomplished when the lidar observations are not considered. It shows the monthly wind shear characteristics are in the agreement with yearly wind turning. In conclusion, all of the comparisons show that the wind shear is in agreement with the turning of the wind.

The findings of this master study help the understanding of wind turning behaviour in the atmosphere. With the growth of wind energy industry and the increasing size of the wind turbines, there is a need for an accurate and detailed description of the wind turning in the first 200 m above the ground.

References

[Age12]   J. M. Agency. *Measurement of Surface Wind*. 2012. URL: http://www.jma.go.jp/jma/jma-eng/jma-center/ric/material/1_Lecture_Notes/CP4-Wind.pdf.

[Amo06]   J. Amouroux, ed. *Green Energy and Technology*. Bentham Science Publishers, July 2006. ISBN: 9781608052851. DOI: 10.2174/97816080528511060101. URL: http://www.benthamdirect.org/pages/content.php?9781608052851.

[Ant00]   D. J. F. Anthoni. Oceanography - currents and circulation (2) (Dec. 2000).

[Ass+09]   E. W. E. Association et al. *Wind Energy-The facts*. Routledge, 2009. ISBN: 978184407710.

[Ass00]   D. W. I. Association. Guided Tour on Wind Energy (Sept. 2000). URL: http://ele.aut.ac.ir/~wind/en/tour/.

[BMN13]   J. Berg, J. Mann, and M. Nielsen. *Notes for DTU course 46100 : Introduction to micro meteorology for wind energy Department of Wind Energy Report 2013*. Vol. 0009. February. DTU Wind Energy, 2013, p. 104. ISBN: 9788792898.

[Car13a]   J.-p. Cariou. Pulsed lidars. **2** (2013), 65–81. URL: http://rasei.colorado.edu/wind-research-internal1/Jean_Pierre_Cariou.pdf.

[Car13b]   J.-P. Carriou. Pulsed coherent lidars for wind remote sensing. June (2013), 1–23.

[Coh+03]   J. Cohen et al. *Applied multiple regression/correlation analysis for the behavioral sciences*. Lawrence Erlbaum Associates, 2003, p. 703. ISBN: 0805822232.

[DN09]   J. Diebel and J. Norda. *Historical Weather For 2009 in Tune near Roskilde, Denmark*. 2009. URL: http://weatherspark.com/history/28829/2009/Tune-near-Roskilde-Region-Zealand-Denmark.

[Dub04]   U. C. Dublin. *The Ekman Spiral*. Dec. 2004. URL: http://maths.ucd.ie/met/msc/fezzik/Phys-Met/Ch05-4-Slides.pdf.

[Etl02]   "Theoretische Meteorologie.pdf". Ed. by P. D. D. Etling. second. Springer-Verlag Berlin Heidelbeerg, 2002, p. 332. ISBN: 978-3-540-75979-9.

[Flo13]   R. Floors. "Boundary-layer wind profile, measurements and theory Risø-PhD-Report". PhD thesis. 2013.

[Hab13]   J. Haby. *Veering and backing wind defined*. 2013. URL: http://www.theweatherprediction.com/habyhints/48/.

[Hun99]   R. S. Hunter. *Wind speed measurement and use of cup anemometry*. 1999.

[LC12]   J. Lundquist and A. Clifton. *How turbulence can impact power performance*. Sept. 2012. URL: https://www.wind-watch.org/documents/how-turbulence-can-impact-power-performance/.

[Peñ09]   A. Peña. "Sensing the wind profile Risø-PhD-Report". PhD thesis. 2009. ISBN: 9788755037090. URL: http://www.risoe.dk/rispubl/reports/ris-phd-45.pdf.

[Phi79]   M. P. M. Philip B Russell Thomas J Swissler. lidar aerosol measurements (1979).

[Rar+09]   E. Rareshide et al. Effects of complex wind regimes on turbine performance Proc. *American Wind Energy Association WINDPOWER Conference (Chicago, IL)* (2009).

[Sat+12]   A. Sathe et al. Influence of atmospheric stability on wind turbine loads. *Wind Energy* (July 2012), n/a–n/a. ISSN: 10954244. DOI: 10.1002/we.1528. URL: http://doi.wiley.com/10.1002/we.1528.

[SM09]   G. Svensson and A. a. M. Holtslag. Analysis of Model Results for the Turning of the Wind and Related Momentum Fluxes in the Stable Boundary Layer. *Boundary-Layer Meteorology* **132**.2 (June 2009), 261–277. ISSN: 0006-8314. DOI: 10.1007/s10546-009-9395-1. URL: http://link.springer.com/10.1007/s10546-009-9395-1.

[Stu88]   R. B. Stull. *An Introduction to Boundary Layer Meteorology*. February. Kluwer Academic, 1988, p. 666. ISBN: 9027727686.

[Sys13]   T. A. L. M. System. *Vertical Motion and Atmospheric Stability*. 2013.

[Wag+09]   R. Wagner et al. The influence of the wind speed profile on wind turbine performance measurements. *Wind Energy* **12**.4 (2009), 348–362.

[WL12]   S. Wharton and J. K. Lundquist. Atmospheric stability affects wind turbine power collection. *Environmental Research Letters* **7**.1 (Mar. 2012), 014005. ISSN: 1748-9326. DOI: 10.1088/1748-9326/7/1/014005. URL: http://stacks.iop.org/1748-9326/7/i=1/a=014005?key=crossref.df26a50fc7064a0a7c4f98db89353d29.

[Yam84]   R. J. Yamartino. A Comparison of Several "Single-Pass" Estimators of the Standard Deviation of Wind Direction. *Climate and Applied Meteorology 23 (9): 1362–1366* (1984).